pH Dependence of the Four Individual Transitions in the Catalytic S-Cycle during Photosynthetic Oxygen Evolution †

ARTICLE *in* BIOCHEMISTRY · MAY 2002

Impact Factor: 3.02 · DOI: 10.1021/bi011691u · Source: PubMed

4 AUTHORS, INCLUDING:

Gábor Bernát
Academy of Sciences of the Czech Republic
31 PUBLICATIONS **450** CITATIONS

SEE PROFILE

pH Dependence of the Four Individual Transitions in the Catalytic S-Cycle during Photosynthetic Oxygen Evolution†

Gábor Bernát,‡ Fatemeh Morvaridi, Yashar Feyziyev, and Stenbjörn Styring*

Department of Biochemistry, Center for Chemistry and Chemical Engineering, Lund University, P.O. Box 124, S-221 00 Lund, Sweden

Received August 20, 2001; Revised Manuscript Received March 5, 2002

ABSTRACT: We have investigated the pH dependence for each individual redox transition in the S-cycle of the oxygen evolving complex (OEC) of photosystem II by electron paramagnetic resonance (EPR) spectroscopy. In the experiments, OEC is advanced to the appropriate S-state at normal pH. Then, the pH is rapidly changed, and a new flash is given. The ability to advance to the next S-state in the cycle at different pHs is determined by measurements of the decrease or increase of characteristic EPR signals from the OEC in different S-states. In some cases the measured EPR signals are very small (this holds especially for the S_0 ML signal at pH >7.5 and pH <4.8). Therefore, we refrain from providing error limits for the determined p*K*'s. Our results indicate that the $S_1 \rightarrow S_2$ transition is independent of pH between 4.1 and 8.4. All other S-transitions are blocked at low pH. In the acidic region, the p*K*'s for the inhibition of the $S_2 \rightarrow S_3$, the $S_3 \rightarrow [S_4] \rightarrow S_0$, and the $S_0 \rightarrow S_1$ transitions are about 4.0, 4.5, and 4.7, respectively. The similarity of these p*K* values indicates that the inhibition of the steady-state oxygen evolution in the acidic range, which occurs with p$K \approx 4.8$, is a consequence of similar pH blocks in three of the redox steps involved in the oxygen evolution. In the alkaline region, we report a clear pH block in the $S_3 \rightarrow [S_4] \rightarrow S_0$ transition with a p*K* of about 8.0. Our study also indicates the existence of a pH block at very high pH (p$K \approx 9.4$) in the $S_2 \rightarrow S_3$ transition. The $S_0 \rightarrow S_1$ transition is not affected, at least up to pH 9.0. This suggests that the inhibition of the steady-state oxygen evolution, which occurs with a p*K* of 8.0, is dominated by the inhibition of the $S_3 \rightarrow [S_4] \rightarrow S_0$ transition. Our results are obtained in the presence of 5% methanol (v/v). However, it is unlikely that the determined p*K*'s are affected by the presence of methanol since our results also show that the pH dependence of the steady-state oxygen evolution is not affected by methanol. The results in the alkaline region are in good agreement with a model, which suggests that the redox potential of $Y_Z^{\bullet}/Y_Z$ is directly affected by high pH. At high pH the $Y_Z^{\bullet}/Y_Z$ potential becomes lower than that of S_2/S_1 and S_3/S_2. The acidic block, with a p*K* of 4−5 in three S-transitions, implies that the inhibition mechanism is similar, and we suggest that it reflects protonation of a carboxylic side chain in the proton relay that expels protons from the OEC.

Photosystem II (PSII)[1] catalyzes the light-driven reduction of plastoquinone. The electrons needed for the reduction come from water that is oxidized to molecular oxygen according to the equation:

$$2H_2O \rightarrow O_2 + 4H^+ + 4e^- \quad (1)$$

Thereby, PSII supplies the biosphere with both electrons from an endless resource and the oxygen needed for respiratory processes in all aerobic life. Water oxidation by PSII is thus one of the key reactions in the biosphere.

The PSII reaction center is a large, multisubunit enzyme (*1*−*4*). It is situated in the thylakoid membrane in oxygen evolving photosynthetic organisms where it spans the membrane from the lumenal to the stromal side. Water oxidation occurs on the lumenal side of PSII and is carried out by a triad (*5*) of highly oxidizing components, which are the primary donor P680, tyrosine$_Z$ (Y_Z) and the Mn_4 cluster. Y_Z and the Mn_4 cluster constitute the catalytic site for water oxidation in the OEC (*3*, *6*−*8*). The donor side triad carries out a sequential series of electron transfer reactions ultimately oxidizing water.

When a photon hits the PSII antenna chlorophylls, the energy is transferred to the primary electron donor P680 that is excited. The excited P680 reduces the acceptor complex

† The financial support from the Knut and Alice Wallenberg Foundation, the Swedish Natural Science Research Council, DESS, the Swedish National Energy Administration, the Sven and Lily Lawski Foundation (F.M.), and the EC Program "Improving Research Potential and the Socio-economic Knowledge Base" (MCFI-200001465) (G.B.) is gratefully acknowledged.

* Corresponding author: phone, +46 46 222 01 08; fax, +46 46 222 45 34; e-mail, stenbjorn.styring@biokem.lu.se.

‡ Permanent address: Institute of Plant Biology, Biological Research Center, Hungarian Academy of Science, P.O. Box 521, H-6701 Szeged, Hungary.

[1] Abbreviations: Chl, chlorophyll; EPR, electron paramagnetic resonance; Hepes, 4-(2-hydroxyethyl)piperazineethanesulfonic acid; Mes, 4-morpholineethanesulfonic acid; ML, multiline (signal); OEC, oxygen evolving complex; P*p*BQ, phenyl-*p*-benzoquinone; PSII, photosystem II; P680, primary donor of PSII; SII_{slow}, the EPR signal from the neutral $Y_D^{\bullet}$ radical; Y_Z and Y_D, redox-active tyrosine residues D1−161 and D2−161 in PSII.

10.1021/bi011691u CCC: $22.00
Published on Web 04/11/2002

Scheme 1

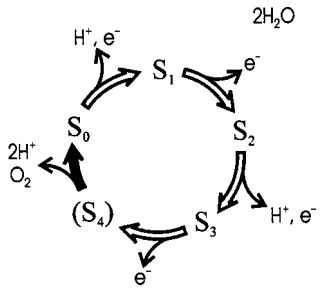

in PSII that is composed of a pheophytin molecule and two quinones (Q_A and Q_B) situated on the stromal side of the membrane. The oxidized primary donor $P680^+$ is rapidly reduced in multiphasic reactions from Y_Z (*3*). This is a pure electron transfer reaction, but at its oxidation Y_Z is deprotonated to a closely lying base D1-His190 (*9*−*14*), resulting in formation of the neutral $Y_Z^\bullet$ radical (*15*−*21*). $Y_Z^\bullet$ is reduced by the Mn_4 complex. Either $Y_Z^\bullet$ is reduced by an electron from the Mn_4 cluster while the proton is returned from D1-His190 (*11*, *22*−*25*; see also ref *26*) or $Y_Z^\bullet$ is reduced by H-atom transfer or proton-coupled electron transfer from the Mn_4 complex (*15*−*23*).

During turnover, the OEC cycles through the S-cycle (*27*) (Scheme 1). The S_0 state is the most reduced state. The S_1 state is one step more oxidized and is the dark stable state. The further sequential removal of three more electrons results in formation of S_2, S_3, and finally the S_4 state. The S_4 state is an unstable, transient state that rapidly releases a molecule of oxygen, resulting in reduction of OEC to the S_0 state.

The oxidation of water to molecular oxygen (eq 1) also involves the release of four protons. These are expelled from PSII on the lumenal side of the complex. Scheme 1 shows one experimentally determined pattern for the H^+ release (*28*, *29*), but this pattern is very preparation sensitive, especially to the integrity of the studied PSII complex (e.g., the presence of extrinsic subunits on the lumen side of PSII) (*30*−*33*). It also varies very much with the measuring pH (*29*, *30*, *32*, *34*, *35*).

It is currently much debated how protons are released from the OEC. Proponents for models where the reduction of $Y_Z^\bullet$ involves H-atom transfer from the Mn_4 cluster argue that the proton is always expelled from Y_Z-OH. The proton release occurs through a hydrogen bond network starting from Y_Z and His190 (*11*, *12*, *14*−*21*, *36*, *37*) and occurs with fast kinetics as Y_Z is oxidized (*30*, *35*, *38*). In contrast, models where reduction of Y_Z from the Mn_4 cluster only involves electron transfer demand that the protons are expelled from the water site in the Mn cluster via ill-defined pathway(s) (*26*, *29*, *39*, *40*). There also exist proposals that protons are expelled from the Mn_4 cluster in some S-transitions and from Y_Z in other S-transitions (*22*−*24*, *41*).

In contrast to the proton release pattern, the overall pH dependence for steady-state oxygen evolution is clear and well described. The oxygen evolution in PSII-enriched membranes is maximal at pH 6.0−7.0 (for example, see refs *42* and *43*). It decreases on the alkaline and the acidic sides with half-inhibition values at pH 4.8−5.5 and 7.4−8.0 (*42*, *43*). It is however not clear which step(s) in the S-cycle is (are) responsible for this inhibition pattern. The pH dependence for an individual S-cycle transition has only been attempted for $S_1 \rightarrow S_2$, which in early work (using small EPR signals) was interpreted to be pH independent between pH 5.5−8.5 (*43*). There also exist other attempts to estimate or discuss the pH dependence of other S-transitions using the oscillation over a flash series of O_2 yield or an S-state related thermoluminescence band as the experimental probe (*44*, *45*). However, in these experiments the pH was always changed already in the S_1 state. Thus, clear results on steps later in the cycle could not be obtained.

In this study, we have measured the pH dependence between pH 4 and pH 9 for each individual S-transition. We have prepared PSII in the S_n state by flashes at 20 °C at pH 6.0. The pH was then rapidly adjusted by a pH jump (*46*, *47*). The ability to advance to the S_{n+1} state was then tested with an additional flash. We have used EPR signals from the S_0, S_2, and S_3 states (*6*, *48*−*57*) and our recently acquired knowledge of their pH dependence (*46*, *47*, *54*) to probe if the transition is functional at a certain pH or not.

MATERIALS AND METHODS

PSII Membrane Preparation. PSII-enriched membrane fragments were prepared according to ref *58* from greenhouse-grown spinach plants cultivated on liquid culture medium. The preparations were stored at −80 °C at approximately 10 mg of Chl/mL. The oxygen evolution was 350−400 μmol (mg of Chl)$^{-1}$ h^{-1}. All chlorophyll determinations were made in 80% acetone (*59*).

Synchronization of PSII and pH-Jump Experiments. For all pH experiments the PSII-enriched membranes were transferred to a low-buffering medium [0.5 mM Mes, 5% methanol (v/v), 400 mM sucrose, 10 mM $MgCl_2$, 10 mM NaCl, 5 mM $CaCl_2$ at pH 6.0] to facilitate the later pH changes (*46*). The samples were filled into calibrated EPR tubes to a final concentration of 3−4 mg of Chl/mL. The purpose of the methanol addition was to allow observation of the S_0 ML EPR signal (*48*, *49*), which was used for the determination of the pH dependencies of two of the four S-transitions (Scheme 2). Also, the S_2 ML signal is larger in the presence of methanol (*60*), which also facilitates our analysis. The addition of 5% methanol is known to have no effect on the steady-state oxygen evolution in PSII (*60*), and our results here also show that methanol addition does not alter the pH dependence of the oxygen evolution (see below).

The membranes were then illuminated with room light at 20 °C for 3 min to oxidize Y_D, and then they were dark incubated for 15 min. PSII was synchronized in the S_1 state by using a preflash protocol followed by a subsequent dark adaptation for 15 min (*61*−*63*). The external electron acceptor P*p*BQ (dissolved in DMSO) was added to a final concentration of 0.5 mM, 1 min before the excitation flashes. The OEC was advanced to the appropriate S-state at pH 6.0 by providing 0 (S_1), 1 (S_2), 2 (S_3), or 3 (S_0) saturating flashes at 20 °C (denoted the *excitation flashes*), given at 5 Hz from a Nd:YAG laser (6 ns, 532 nm, 350 mJ).

After the excitation flashes, the pH of the medium was adjusted by addition of a stronger buffer in the range of pH 3.75−9.5 (10% v/v) added and quickly mixed (10−30 s) with a Hamilton syringe equipped with a spiral-shaped tip. The buffers used were DL-glutamic acid/KOH (pH 3.75−5.0), Mes/KOH (pH 5.0−7.0), Hepes/KOH (pH 7.0−8.0), and glycylglycine/KOH (pH 8.0−9.5) (*46*). The final buffer

Scheme 2

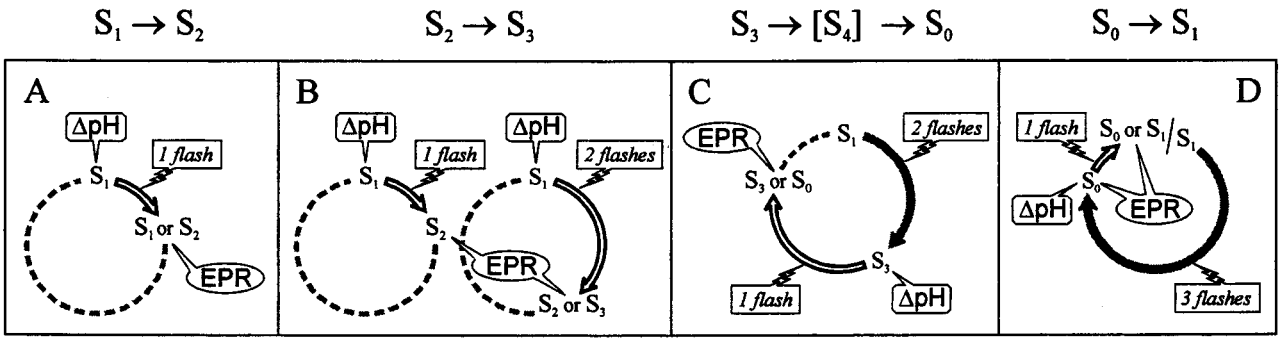

concentration was 14 mM. The EPR samples were either frozen at this level of sample preparation (to obtain control samples prior to the probe flash) or exposed to one more laser flash, the *probe flash*, provided immediately after the pH jump. In the latter case, the samples were frozen within 1−2 s after the flash. The probe flash was provided at 20 °C.

Experimental Protocol and Data Analysis for the $S_1 \rightarrow S_2$ Transition. To study the $S_1 \rightarrow S_2$ transition, the formation of the S_2 ML signal was followed. In these experiments the samples were frozen after the pH jump and the probe flash (Scheme 2, panel A). The probe flash was provided less than 5 s after the pH change was completed.

The S_2 ML signal was recorded after the probe flash, and the signal intensity was estimated by the sum of three hyperfine lines as indicated in Figure 1 (*48*). The spectra were normalized to SII_{slow}, the radical EPR signal from the neutral $Y_D^\bullet$ radical, which was used as an internal standard to quantify the amount of PSII centers in the sample (see below, EPR section). No other corrections were necessary in this experiment.

The pH dependence of the $S_1 \rightarrow S_2$ transition was estimated from the fraction of the PSII centers that reached the S_2 state with the probe flash. This fraction was determined from the amplitude of the S_2 ML signal obtained at different pHs. However, we earlier found that the amplitude of the S_2 ML signal is pH dependent (*46*). We used this knowledge to estimate the pH dependence of the $S_1 \rightarrow S_2$ transition by the division of the normalized amplitudes of the S_2 ML signal at different pHs with the titration curve of the amplitude of the S_2 ML EPR signal. This titration curve was originally published in ref *46*. In our earlier work (*46*) the S_2 state was exposed to the modified pH for 30 s. At elevated pH, these 30 s cause a significant decay of the S_2 state. In our present work, the S_2 state was only exposed to the modified pH for 1−2 s (the time between the probe flash and the freezing of the EPR sample). In our analysis, we therefore corrected our earlier titration curve for the amplitude of the S_2 ML signal using newly acquired data for the pH-dependent decay of the S_2 ML signal (this work, Figure 2A, inset).

To demonstrate the reliability of this signal amplitude correction, we also applied an alternative approach. In this experiment the pH was moved back to pH ≈6.0 after the probe flash had been given. These reversibility experiments were achieved by the addition of 10% (v/v) 400 mM Mes/KOH at pH 5.75 (if the initial pH = 4.1) or 6.25 (pH = 8.0). EPR spectra were recorded either directly after the probe flash (at pH 4.1 or 8.0) or after the pH reversal (to pH ≈6.0). In this protocol the amplitude of the S_2 ML signal measured after the pH reversal directly indicated how much S_2 state was indeed formed by the probe flash. The two alternative protocols gave identical results.

Experimental Protocol and Data Analysis for the $S_2 \rightarrow S_3$ Transition. In the studies of the $S_2 \rightarrow S_3$ transition we followed the disappearance or decrease of the S_2 ML signal after the probe flash (Scheme 2, panel B). Two parallel sample series were prepared. The pH was changed in the S_1 state. Then, the samples were frozen after either one or two probe flashes (Scheme 2, panel B). The probe flash(es) was (were) provided less than 5 s after the pH change in S_1 was completed. The S_2 ML signal intensity was estimated and then normalized to $Y_D^\bullet$ and to the various pHs as described for the $S_1 \rightarrow S_2$ transition.

It is important to note that this experimental design was based on our observation that the $S_1 \rightarrow S_2$ transition was pH independent (see Results). Thus, it was possible to study the $S_2 \rightarrow S_3$ transition in samples where the pH was changed already in the S_1 state. We also attempted to study the $S_2 \rightarrow S_3$ transition in samples where the pH jump was performed in the S_2 state, but this experiment proved to be imprecise due to the pH-dependent decay of the S_2 state, which complicated our analysis.

The efficiency of the $S_2 \rightarrow S_3$ transition at different pHs was calculated by comparison of the fraction of PSII centers present in the S_2 state in the parallel samples from the one- and two-flash series. The principle in the experiment was that the S_2 state population obtained by the first flash (at a certain pH) diminished following the second flash if $S_2 \rightarrow S_3$ was functional. If $S_2 \rightarrow S_3$ was inhibited, the S_2 population remained (it could even have increased if the block was total) after the second flash. Our detailed analysis was based on the equation:

$$[S_2]_{2fl} = (100 - [S_2]_{1fl})(1 - \alpha) + [S_2]_{1fl}x + [S_2]_{1fl}(1 - x)\alpha \quad (2)$$

where $[S_2]_{1fl}$ and $[S_2]_{2fl}$ are the S_2 state populations (in percent) after one and two flashes, respectively. α is the miss parameter of the series, determined by the equation

$$[S_2]_{1fl} = 100(1 - \alpha) \quad (3)$$

and x is the "block" parameter. Thus, the efficiency of the transition corresponds to $(1 - x)$. The efficiency of the transition was depicted as a function of pH and was fitted with a bell-shaped titration curve with two pK's (eq 5 in ref *46*).

Experimental Protocol and Data Analysis for the $S_3 \rightarrow S_0$ Transition. In the studies of the $S_3 \rightarrow S_0$ transition the formation of the S_0 population or the disappearance of the S_3 population was followed by two different experimental protocols.

In the former case the formation of the S_0 ML signal was measured in the samples which were frozen after the pH jump and the probe flash (Scheme 2, panel C). The probe flash was given 30 s after the last excitation flash.

To decrease the S_2 ML signal contribution in the EPR spectra after the probe flash, 4 min dark incubation was applied at room temperature between the probe flash and freezing of the EPR sample. This allows quite efficient decay of any S_2 and S_3 centers (remaining after the flashes) without affecting the S_0 population too much. Thus, this treatment reduces the S_2 ML signal, which would otherwise complicate our analysis of the S_0 ML spectra (*46*, *48*, *51*).

The raw spectra were normalized to SII_{slow}. Then, any remaining S_2 ML signal contribution was subtracted. The intensity of the S_0 ML signal, which now dominated the spectra, was estimated by the sum of three hyperfine lines as indicated in Figures 5 and 8 (*48*). These intensities were corrected for the small decay of the S_0 ML signal, which occurred during the 4 min dark incubation, using stability data for the S_0 state at different pHs from ref *42*.

The efficiency of the $S_3 \rightarrow S_0$ transition was calculated from these corrected S_0 ML signal intensities. However, similar to the S_2 ML signal, the amplitude of the S_0 ML signal is pH dependent (*46*). To determine the fraction of PSII that reached the S_0 state with the probe flash, it was necessary to correct the amplitude of the S_0 ML signal for this pH dependence. Therefore, the corrected S_0 ML amplitudes were divided by the bell-shaped pH dependence curve of the intensity of this signal (*46*). The p*K*'s of the inhibitions of this transition were then estimated as described in the section about the $S_2 \rightarrow S_3$ transition.

We also applied an alternative experiment to investigate the $S_3 \rightarrow S_0$ transition. Here, the disappearance of the S_3 population was directly followed by measurements of the $S_2Y_Z^{\bullet}$ signal that can be induced from the S_3 state at high pH (*47*). In these experiments, a second pH jump to pH 8.3 [achieved by the addition of 10% (v/v) 400 mM glycylglycine at pH 8.5] was applied immediately after the probe flash, before the samples were frozen. This second pH jump was performed to make the $S_2Y_Z^{\bullet}$ split signal detectable from any centers that were left in the S_3 state after the probe flash. The time interval between the flashes was as described above. The samples were frozen directly after the second pH jump, which immediately followed the probe flash. Thus, in this experiment we did not wait 4 min after the probe flash. The amplitude of the split signal was measured as in ref *47*.

Experimental Protocol and Data Analysis for the $S_0 \rightarrow S_1$ Transition. In the studies of the $S_0 \rightarrow S_1$ transition two different protocols were applied, depending on the pH interval studied.

At acidic and neutral pHs the disappearance or decrease of the S_0 ML signal was followed. First, the S_0 state was formed by three flashes. Then, 4 min dark incubation was applied to allow S_2 ML signal decay. Thereafter, the pH was changed, and the first EPR spectra were recorded to estimate the S_0 ML signal at the various pHs. Then, the sample was thawed to 20 °C (30 s), and the probe flash was given (Scheme 2, panel D). A second dark incubation step (4 min) was applied before the samples were frozen, and the second set of EPR spectra was recorded.

Table 1: Distribution of the S-State Population after 0−4 Saturating Flashes at pH 6.0[a]

flash no.	"S-state"[b]	S_1 (%)	S_2 (%)	S_3 (%)	S_0 (%)
0	S_1	100[c]	0	0	0
1	S_2	15	85	0	0
2	S_3	2	26	72	0
3	S_0	0	6	33	61
3[d]	S_0	nd	nd	<8[e]	58
4[d]	S_1	nd	nd	nd	<15

[a] Obtained from the oscillation of the S_2 and S_0 state ML signals. The miss factor, α, was ≈0.15. [b] Dominant S-state. [c] The samples are synchronized in the S_1 state (see Materials and Methods). [d] With 4 min dark adaptation after the third flash (see Materials and Methods). [e] Calculated from the lifetime of the S_3 state determined by Styring and Rutherford (*61*).

The raw spectra were subjected to the same data handling protocol as described for the spectra in the $S_3 \rightarrow S_0$ transition studies (see above) except for the correction of the pH-dependent decay of the S_0 ML signal, which was unnecessary for two reasons. First, the initial 4 min dark incubation was applied at pH 6.0 for all samples. Thus all of the control samples represent the same S_0 population irrespective of the final measuring pH. Second, no S_0 ML EPR signal was detected between pH 6.2 and pH 7.5 after the probe flash (thus, there was no signal to be corrected). Below pH 6.0, the S_0 decay is very slow, and the S_0 population hardly changes during the 4 min dark incubation period (*42*).

The efficiency of the $S_0 \rightarrow S_1$ turnover at low and neutral pHs is calculated from the relative decrease of the S_0 ML signal intensities after the probe flash. The calculated, pH-dependent efficiency of the $S_0 \rightarrow S_1$ transition at acidic and neutral pHs was fitted by a single p*K* (eq 1 in ref *47*).

At alkaline pHs the S_0 signal is small and difficult to measure with precision. However, in the studies of the $S_0 \rightarrow S_1$ transition a complementary technique with parallel samples could be applied above pH 7.0. In these studies, the formation of the S_1 population was detected instead of the disappearance of the S_0 population. In the experiments, one sample was frozen before and one after the probe flash at each pH. The probe flash was given 30 s after the last flash of the exciting flash series. The samples were then given an additional illumination at 200 K after the cursive probe flash. Illumination at 200 K allows the $S_1 \rightarrow S_2$ transition in the OEC (*61*, *65*). Thus, if S_1 centers are present after the probe flash, they will be quantitatively converted to the S_2 state. Consequently, comparison of the S_2 ML signal intensities before and after illumination at 200 K provided a measure of the S_1 population formed by the probe flash. The S_2 population was in each case estimated from the corrected S_2 ML signal amplitude titration curve (see the text concerning the $S_1 \rightarrow S_2$ transition and ref *46*).

Characterization of the Sample Series and the Individual Samples. The flash-dependent S-state distribution of the samples (Table 1) was calculated from the miss factor parameter *in each individual series*. This parameter was determined by the flash-number dependent oscillations of S_2 and S_0 state ML signals over a flash sequence (*46*, *48*, *51*, *62*, *63*). When the EPR measurements were finished, the

samples were thawed, and the final pH, steady-state O_2 evolution at pH 6.0 (*46*, *47*), and Chl concentration were determined.

EPR Spectroscopy. Low-temperature continuous-wave EPR measurements were performed with an ESP500e spectrometer using a SuperX EPR049 microwave bridge and an ER4122SHQ cavity (Bruker Analytik GmbH, Karlsruhe, Germany). The system was fitted with a liquid helium cryostat and temperature controller from Oxford Instruments Ltd. (Oxon, U.K.). Spectrometer settings are given in the figure legends.

SII_{slow}, the EPR signal from the tyrosyl$_D$ radical ($Y_D^\bullet$), was used as the internal standard in all experiments. Our preillumination protocol (3 min at 20 °C using room light) is known to oxidize all Y_D to its radical state. At normal pHs, $Y_D^\bullet$ is very stable, and after our preflash and dark adaptation procedure it is safe to assume that $Y_D^\bullet$ amounts to 1 radical per PSII center (*3*, *42*, *53*, *62*) before pH jump and flash protocol. In most experiments the pH jump and the flashing took about 30 s, but in some studies we applied 4 min dark adaptation prior to freezing (see above). This is short enough that decay of $Y_D^\bullet$ can be neglected at all pHs <7.7. At the very high pHs, however, $Y_D^\bullet$ might decay somewhat. It was therefore not used as a standard here, but other suitable internal standards are difficult to envisage. Therefore, we used the mean integral for $Y_D^\bullet$ in all samples between pH 4.0 and pH 7.7 in the particular experimental series (5−15 samples) as an internal standard in samples at pH >7.7.

Steady-State O_2 Evolution. Steady-state O_2 evolution was measured with a Clark-type oxygen electrode (Hansatech, Pentney, U.K.) at 20 °C in a medium containing 20 mM Mes, 10 mM $MgCl_2$, 10 mM NaCl, 5 mM $CaCl_2$, and 400 mM sucrose. The measurements were made in either the absence or presence of 5% (v/v) methanol. The pH of the buffer used was adjusted before the measurements. P*p*BQ (in DMSO; 0.5 mM final concentration) was added as an external acceptor. Illumination was supplied from a saturating white light source filtered by an OG590 orange glass filter (Schott, Mainz, Germany). The final pH was measured in the O_2 cell after the measurements.

RESULTS

S-State Distribution as a Function of the Number of Flashes. Our intention was to study the pH dependence of each S-transition individually and to minimize the interference with possible pH-induced blocks from the other S-transitions. Therefore, it was inappropriate in this study to cycle through the entire S-cycle at each pH. Instead, only the S-transition in question was carried out at the modified pH.

To accomplish this, we first exposed PSII membranes (with OEC synchronized in the S_1 state by a preflash protocol; see Materials and Methods) to 0−3 powerful laser flashes at pH 6.0. After the flashes the pH was rapidly changed, and a new flash (the probe flash) was given. The S-state advancement at different pHs was determined by measurements of the decrease or increase of the characteristic EPR signals from different S-state populations after the probe flash. We followed the changes of the S_0 state (for the $S_3 \rightarrow [S_4] \rightarrow S_0$ and $S_0 \rightarrow S_1$ transitions) and the S_2 state (for the $S_1 \rightarrow S_2$ and $S_2 \rightarrow S_3$ transitions) by measuring the S_0 and S_2 ML EPR signal intensities, respectively (Scheme 2).

Table 1 shows the S-state distribution in our samples after 0−4 flashes, which was determined from oscillations of the S_0 and S_2 ML EPR signals. The miss factor in these experiments was about 15%, determined in many series at pH 6.0. Our flash protocol using the preflash technique makes it possible to reach 85% S_2, 72% S_3, and 61% S_0, after one, two, and three flashes, respectively.

The miss factor is considered to be S-state and pH dependent (*13*, *44*). Despite this, we used the same average miss parameter (≈15%) over the whole pH range between 4.0 and 9.0. The reason for this is that the effect of an altered miss factor or an acidic or alkaline block is the same: the transition does not work. The exact value of the miss factors (if this is S-state dependent) for the particular S-transition has little importance when the $S_1 \rightarrow S_2$ and $S_3 \rightarrow [S_4] \rightarrow S_0$ transitions are investigated since the S_2 and S_0 populations increased from zero after the probe flash. Contrary to this, the miss parameters were of greater importance in studies of the $S_2 \rightarrow S_3$ transition, where, as a consequence of the misses, a significant S_2 population (≈25%) was still present after the second flash (see Materials and Methods).

pH Dependence of the $S_1 \rightarrow S_2$ Transition. In this experiment we changed the pH in the S_1 state before the probe flash was given and the sample was frozen (Scheme 2, panel A). The left panel in Figure 1 shows the S_2 ML EPR signal formed at three different pHs. At pH 6.0 (spectrum b), where PSII is fully functional, we observe a large S_2 ML signal. The signal is significantly smaller at both low (spectrum a) and high (spectrum c) pH. The appearance of the S_2 ML signal even at pH 4.1 and 8.0 reveals that the $S_1 \rightarrow S_2$ transition is partially or totally open between these pH values.

Figure 2A (data points) shows the amplitude of the S_2 ML signal formed between pH 4.1 and pH 8.4. The thick line shows the fit of the data points to two p*K*'s (*46*). At first glance it seems that the formation of S_2 is inhibited at both high and low pH. *However, this is not the case*. The S_2 ML signal data in Figure 2A need more careful interpretation.

We recently found that the amplitude of the S_2 ML signal was pH dependent (*46*, *54*). The S_2 ML signal amplitude decreased at low and high pH with p*K*'s of 4.5 ± 0.1 and 7.6 ± 0.1 without affecting the actual population of the S_2 state. It is necessary to account for this pH-dependent amplitude change in the evaluation of the data points in Figure 2A.

There is, however, one very important difference between our experiments here and those of Geijer et al. (*46*). Here, we change the pH in the S_1 state; then we flash and freeze within 1 s after the flash. Thus, the S_2 state is never exposed for extreme pHs more than 1−2 s. In contrast, Geijer and co-workers (*46*) changed the pH in the S_2 state which was exposed for extreme pHs for 30 s. The decay of S_2 is pH dependent and faster at elevated pH (*44*). The inset in Figure 2A shows a measurement of the pH-dependent decay of S_2 during 30 s incubation. At pH >7.8, the decay is so fast that it substantially affects the interpretations from our earlier study. In the final analysis this pH-dependent decay was taken into account. For example, at pH 8.4 almost 60% of the S_2 state had decayed during the 30 s mixing time in our original study (*46*; compare with inset in Figure 2A) while

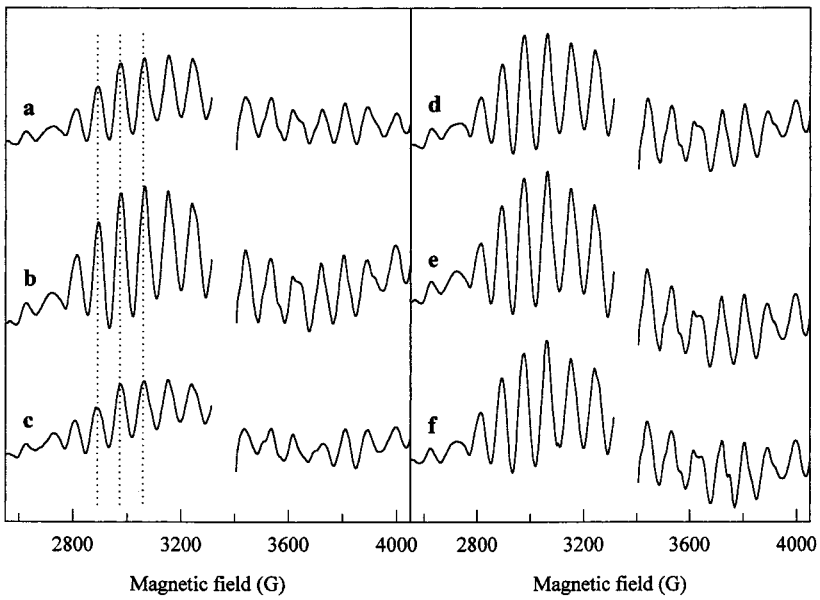

FIGURE 1: S_2 state ML EPR signal induced by one saturating laser flash given *after* the pH jump to (a, d) pH 4.1, (b, e) pH 6.0, and (c, f) pH 8.0. The samples were frozen immediately after the flash (a−c) or were subjected to a second pH change to pH 6.0 (d−f). The dotted lines indicate the three peaks used to determine the spectral intensity of the signal. The radical EPR signal from $Y_D^{\bullet}$ at $g \approx 2$ has been excised for clarity. EPR settings: microwave power 12 mW; microwave frequency 9.41 GHz; temperature 7 K; modulation frequency 100 kHz; modulation amplitude 15 G.

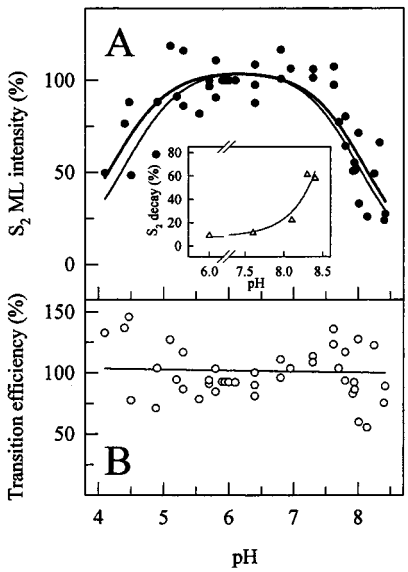

FIGURE 2: pH dependence of the $S_1 \rightarrow S_2$ transition. (A) pH dependence of the S_2 ML signal intensity. The S_2 ML signal was induced by one saturating laser flash given *after* the pH jump (compare Figure 1). The experimental ML signal intensity (●) corresponds to the sum of the amplitudes of the three peaks in the S_2 ML signal indicated by dotted lines in Figure 1. The thick line represents the fit of the experimental points with two p*K*'s (*46*). The thin line represents the titration curve of the S_2 ML signal amplitudes, taken from ref *46* and corrected by the time-dependent decay of the S_2 ML signal (see inset and text for explanation). The corrected titration curve has two p*K*'s of 4.4 ± 0.1 and 8.0 ± 0.1, respectively. Inset: pH dependence of the decay of the S_2 ML signal during a 30 s incubation at room temperature. (B) Efficiency of the $S_1 \rightarrow S_2$ transition as a function of pH. The data points (○) are obtained from panel A by division of the experimental points (●) with the decay-corrected titration curve of the S_2 ML signal (panel A, thin line). The line represents a fit of the data points (○) with a parabolic function indicating that there is no pH dependence in the transition.

the decay was very small (≈5%) in our present study. This forced us to recalculate the titration curve from Geijer et al. (*46*) to our present conditions. The recalculation was carried out by correcting the S_2 ML intensities on the titration curve from ref *46* with the fraction of the signal that decays during the 30 s incubation period (this work, Figure 2A, inset). This resulted in an increase of the alkaline p*K* in the titration curve from 7.6 (in ref *46*) to 8.0 ± 0.1 while the acidic p*K* was hardly affected.

In Figure 2A, the thin line shows the recalculated titration curve from Geijer et al. (*46*) when the decay of the S_2 state at high pH is taken into account. It is clear that our measured amplitudes (Figure 2A, fitted with the thick line) are very similar to the corrected curve from Geijer et al. (Figure 2A, thin line). This shows that the same amount of S_2 is formed by a flash at every pH. In other words, the $S_1 \rightarrow S_2$ transition is pH independent over the pH range 4.1−8.4 (Figure 2B; see also Table 2).

The results presented in Figure 2 indicate that the $S_1 \rightarrow S_2$ transition is pH independent between pH 4.1 and pH 8.4. However, the analysis depends entirely on comparison with our earlier pH titration curve for the amplitude of the S_2 multiline signal amplitude. This was obtained by performing the pH jump in the S_2 state, and not like here in the S_1 state, and it might be argued that the experiment is too different to allow this comparison without further controls. We therefore performed an alternative experiment to test wether the S_2 state really was formed to a large extent by a flash given at all studied pHs. In this experiment (Figure 1, left panel) we changed the pH in the S_1 state; then the sample was exposed to the probe flash and the EPR spectra were recorded. In a parallel sample, the pH was adjusted back to ≈6 directly after the flash. Then the EPR was measured. Figure 1 shows the EPR spectra obtained by such an experiment. When the flash was given at pH 4.1 or pH 8.0, the S_2 multiline signal was much smaller than when the flash was given at pH 6.0 (Figure 1, left panel). However, in the parallel samples, where the pH was changed back to pH 6.0 *after* the flash, the signal amplitude increased in the samples

that were flashed at pH 4.1 and 8.0 (Figure 1, right panel). At both pHs the signal increased to an amplitude comparable in size to the signal recorded in a parallel sample that was exposed only to pH 6.0 (Figure 1, spectrum e). This shows that the same amount of the S_2 state was indeed formed by the flash irrespective of the pH. After flashes at low and high pH the final multiline signal amplitude was always somewhat smaller than at pH 6.0. The reversal of the signal amplitude by the pH shift from low pH encompassed 83% of the centers that were in the S_2 state. At basic pH, the reversal encompassed nearly all available centers in the S_2 state since we obtained 93% of the reference (spectrum e) amplitude after the pH change from 8.0 to 6.0. This means, by taking into account the decay of the S_2 ML signal amplitide during the 10 s incubation period (7%), that we formed about 100% S_2 by the probe flash at pH 8.0. The reversibility of the decrease of the S_2 state multiline signal amplitude at high and low pH is higher than in our earlier work (ref *46*, Figure 6A,B). This is due to the very short incubation time at the extreme pHs in the present experiment (10 s compared to 30−60 s in our earlier work) and using a more simple protocol (without sequential sample thawing) which minimizes the pH-dependent decay of the S_2 state.

Thus we conclude that the experiment presented in Figure 1 (right panel) further strengthens our conclusion that the $S_1 \rightarrow S_2$ transition is pH independent between pH 4.1 and pH 8.4. If there are any pH-dependent blocks of this step, the p*K* is <2.5 at the acidic side or >9.5 at the alkaline side, respectively. The experiment also lends further support to our original conclusion (*46*) that it is the amplitude of the S_2 state multiline signal that is pH dependent; it is not the S_2 state that is lost during short exposures to extreme pHs.

Our results that the $S_1 \rightarrow S_2$ transition is pH independent between pH 4.1 and pH 8.4 but that the amplitude of the S_2 ML is pH dependent extend earlier work and clarify some disagreement in the literature. Damoder and Dismukes (*43*) found the induction of the S_2 ML signal to be pH independent between pH 5.5 and pH 8.5. In contrast, Cole et al. (*64*) found two effects at elevated pH when samples were incubated for 1 h on ice. First, they observed a smaller amplitude of the S_2 ML induced by illumination at 200 K above pH 6.8. Second, they observed that this decrease partially was due to irreversible destruction of OEC above pH 8.0.

In essence our results (this study and ref *46*) agree and extend the work by Cole et al. (*64*). We also find that OEC partially is irreversibly destroyed at pH >8.0 [1−2 min incubation at 20 °C results in ≈20% decrease of the O_2 evolution (*46*)] while 15−30 s incubation at high pH (pH <9.0) has little effect (*46*). It should be emphasized that the O_2 evolution at pH 6.0 was measured in every single EPR sample when the EPR analysis was finished. This was done both here and in our earlier work (*46*), and results from samples with severe loss of O_2 evolution were discarded.

We also find the decrease in the formation of the S_2 ML amplitude at high pH, but our investigations in the S_2 state (*46*) show that the signal is decreased due to pH effects on the S_2 state not due to inhibition of the $S_1 \rightarrow S_2$ transition. Cole et al. (*64*) were not aware of this effect. Damoder and Dismukes (*43*) claim that the $S_1 \rightarrow S_2$ transition is functional at pH <8.5 (similar to our conclusion) since their observed S_2 ML signal is similar at neutral and evaluated pH (the S_2 ML signal was induced by illumination at 200 K). It is not clear why their result differed from ours (ref *46* and this study) and Cole et al. (*64*). One possible reason is that the reported spectra [S_2 ML signals are shown only at pH 5.5 and 7.3 (*43*, Figure 1)] are much smaller that those reported by Cole et al. (*64)* or used by us (ref *46* and this study), which might have made quantification of the signal amplitude decrease less obvious.

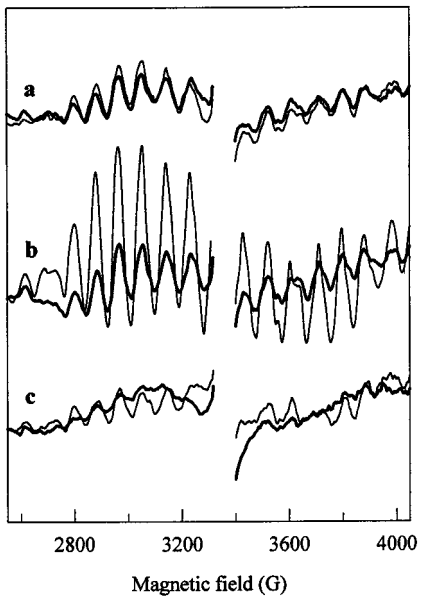

FIGURE 3: S_2 state ML EPR signal induced by one flash (thin lines) or remaining after two (thick lines) flashes given *after* the pH change at (a) pH 3.9, (b) pH 6.2, and (c) pH 8.7. The signal from $Y_D^{\bullet}$ at $g \approx 2$ has been excised for clarity. EPR settings as in Figure 1.

pH Dependence of the $S_2 \rightarrow S_3$ Transition. Since the $S_1 \rightarrow S_2$ transition proved to be pH independent between pH 4.1 and pH 8.4 (see above), it was possible to study the pH dependence of the $S_2 \rightarrow S_3$ transition by a pH adjustment in the S_1 state followed by one or two flashes (Scheme 2, panel B). This has the advantage that we can avoid any decay of the S_2 state during the pH jump, which otherwise would occur rapidly (especially at high pH). Figure 3 shows the results of these experiments at three different pH values. At normal (spectra b, pH 6.2), low (spectra a, pH 3.9), and high pH (spectra c, pH 8.7), the pH-dependent S_2 ML signal intensity achieved by one flash (thin line spectra) was significantly decreased by the second flash (thick line spectra). This shows that the S_2 state formed by the first flash (giving rise to the ML signal) is converted to the S_3 state (no ML signal). The relative decrease of the signal was biggest at pH 6.2 (Figure 4A), which indicates partial blocks at low and high pH during the $S_2 \rightarrow S_3$ transition.

To determine the p*K*'s for the inhibition, the "block factor" was determined using eqs 2 and 3. This evaluation takes into account that there are three S_2 populations with different origin after the second flash. The first part is formed by S_2 centers which did not form S_3 due to block at acidic or alkaline pH (0% when the transition is open, $0\% < x < 72\%$ when the transition is blocked). The second S_2 fraction is turned over from S_1 centers which were *not* turned over to S_2 on the first flash ($15\% \times 0.85 \approx 13\%$; see Table 1). Finally, the third part is formed by S_2 centers, which were in S_2 after the first flash but did *not* turn over to S_3 due to the misses ($85\% \times 0.15 \approx 13\%$; see Table 1).

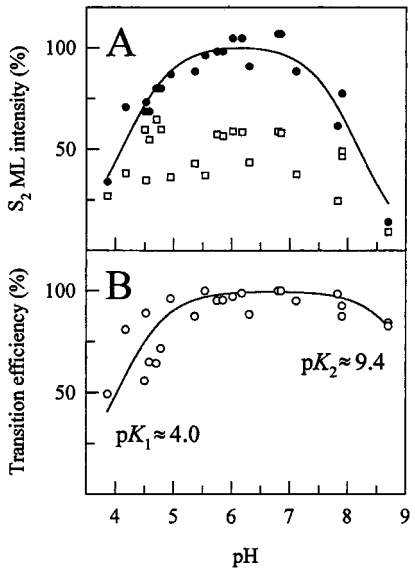

FIGURE 4: pH dependence of the $S_2 \rightarrow S_3$ transition. (A) pH dependence of the S_2 ML signal intensity. The S_2 ML signal was induced by one (●) or remained after two (□) flashes given *after* the pH change. The amplitudes were measured and compared as in Figures 1 and 2A. The line shows the decay-corrected titration curve of the amplitude of the S_2 ML signal derived as described in Figure 2A. (B) Efficiency of the $S_2 \rightarrow S_3$ transition as a function of pH, calculated by eqs 2 and 3 (○) (see text for details). The points were fitted with a titration curve (solid line, fitted by eq 5 from ref *46*) with p*K*'s of about 4.0 and 9.4.

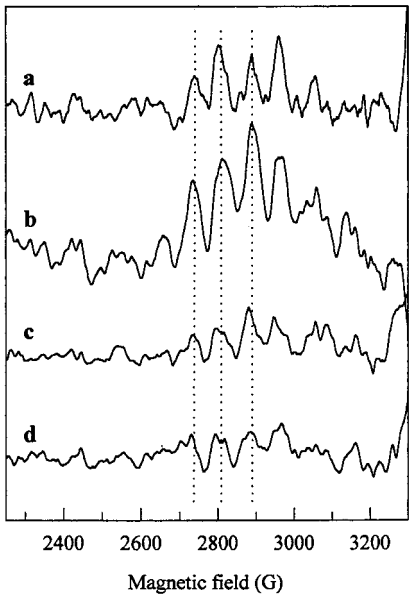

FIGURE 5: Low-field region of the S_0 state ML EPR signal induced by two saturating laser flashes at pH 6.0 followed by the pH jump and the subsequent probe flash. The final pH was (a) pH 4.8, (b) pH 6.2, (c) pH 7.3, and (d) pH 8.0. A 4 min dark incubation was applied before the samples were frozen to minimize the contribution of the S_2 ML signal. Any remaining S_2 ML signal has been subtracted from the EPR spectra. (For raw spectra see Supporting Information.) The dotted lines indicate the three peaks used for the determination of the spectral intensities in Figure 6A. EPR settings: microwave power 50 mW; microwave frequency 9.41 GHz; temperature 7 K; modulation frequency 100 kHz; modulation amplitude 15 G.

The efficiency of the $S_2 \rightarrow S_3$ transition was calculated at all pHs from the S_2 ML signal intensities after one and two flashes and the exact miss factor of the examined series. The results are shown in Figure 4B, which shows that the $S_2 \rightarrow S_3$ transition is totally open between pH 5.0 and pH 8.0 and partially inhibited below and above these values. Fitting the transition efficiency with two p*K* values (*46*) revealed that this transition is inhibited with p$K \approx 4.0$ in the acidic range (Table 2). There also seems to be a weak inhibition at high pH. The approximate p*K* is 9.4 (Table 2). However, the exact titration point for this alkaline block is not possible to determine with precision. The reasons for this uncertainty are twofold. First, we cannot study the transition at pH >9 since the OEC is quickly inactivated at such high pHs. Thus, if there really occurs a block with p$K \approx 9.4$, we can only observe a fraction of this block in our available pH range. Second, at pH 8.8−9.0, even the S_2 ML signal is small, which decreases the precision in our measurement.

It should be noted that we studied the $S_2 \rightarrow S_3$ transition using our knowledge that $S_1 \rightarrow S_2$ is fully open in the entire pH range. This allowed us to alter the pH already in the S_1 state. However, we also attempted to study the $S_2 \rightarrow S_3$ transition by changing pH in the S_2 state (15 s mixing was applied). This experiment proved to be impossible at pH >7.7 due to the fast decay of S_2 at elevated pH (Figure 2, inset), which leads to severe scrambling of the S-states during the mixing period and the subsequent probe flash.

Unfortunately, it was also impossible to obtain high-quality data in the acidic region for similar reasons, i.e., severe scrambling of the S-states during the pH jump. However, at pH 4.0 and 4.5 the S_2 ML signal actually increased on the second flash (not shown). This shows that the S_2 state did not turn over to S_3 at low pH while centers remaining in the S_1 state formed S_2 on the probe flash. We were unable to determine a p*K* from this experiment, but the data qualitatively supported the results presented in Figure 4.

It is noteworthy that we find that $S_2 \rightarrow S_3$ is fully functional at least up to pH 8.0 (Figure 4B). We found this in an experiment where the pH jump was performed already in the S_1 state. Thus, if there had been any inhibition in the $S_1 \rightarrow S_2$ transition, this would have been revealed also in the analysis of the $S_2 \rightarrow S_3$ data. Consequently, the results in Figure 4B support our conclusion that $S_1 \rightarrow S_2$ transition is fully operational up to pH 8.0.

pH Dependence of the $S_3 \rightarrow [S_4] \rightarrow S_0$ Transition. The recent determination of the pH dependence of the S_0 ML signal amplitude (*46*) made similar pH studies on the $S_3 \rightarrow [S_4] \rightarrow S_0$ and on the $S_0 \rightarrow S_1$ transitions possible. The principles of the measurements were similar as applied in our measurements of the $S_1 \rightarrow S_2$ and $S_2 \rightarrow S_3$ transitions.

In the study of the pH dependence of the $S_3 \rightarrow [S_4] \rightarrow S_0$ transition two flashes were given before the pH change, which was followed by the probe flash (Scheme 2, panel C). The probe flash was followed by a 4 min dark incubation to allow decay the S_2 ML signal that otherwise interferes with the S_0 ML signal spectra, making the analysis difficult. Four representative spectra are shown in Figure 5. At pH 6.2 (spectrum b) the S_0 ML signal has its maximal amplitude while the signal intensity was much smaller at pH 4.8 (spectrum a) and pH 7.3 (spectrum c) and even smaller at pH 8.0 (spectrum d).

Figure 6A shows the relative amplitude of the S_0 ML signal as a function of pH. Fitting of these points with two p*K*'s (*46*) resulted in a bell-shaped titration curve (thick line). This titration curve is significantly narrower than the curve

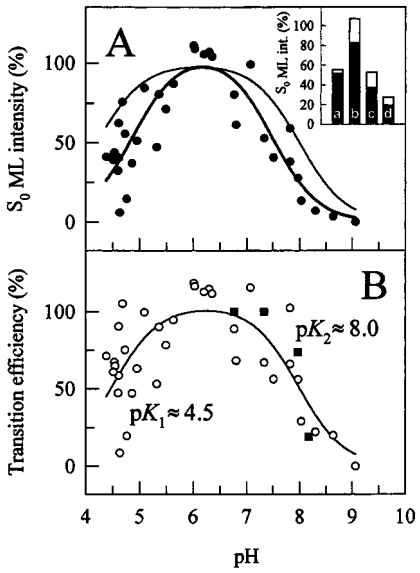

FIGURE 6: pH dependence of the $S_3 \rightarrow [S_4] \rightarrow S_0$ transition. (A) pH dependence of the S_0 ML intensity. The S_0 ML signal was induced by two flashes. These were followed by the pH jump and a probe flash. The plotted S_0 ML signal intensity (●) corresponds to the sum of the amplitudes of three peaks in the S_0 ML signal (dotted lines in Figure 5), corrected for the decay of the S_0 state during the 4 min dark incubation that was applied after the probe flash (see inset and text for explanation). The thick line represents a fit of the experimental points with a titration curve with two p*K*'s (see eq 5 in ref *46*). The thin line shows the titration curve of the amplitude of the S_0 ML signal from ref *46*. Inset: the pH-dependent decay of the S_0 ML signal during the 4 min dark incubation at (a) pH 4.8, (b) 6.2, (c) 7.3, and (d) pH 8.0. The measured signal intensities (black columns) were completed by the calculated decayed fraction (white columns) of the signal. The S_0 lifetimes at different pHs are taken from ref *42*. The plotted points (●) in (A) represent the sum of the black and white columns. (B) Efficiency of the $S_3 \rightarrow [S_4] \rightarrow S_0$ transition as a function of pH. One set of the data points (○) represents the efficiency of formation of the S_0 state at different pHs which was calculated by the division of the data points (●) from panel A and the titration curve of the S_0 ML signal amplitude (panel A, thin line). The second set of the points (■) is taken from an alternative experiment targeting the relative decrease of the S_3 population after the probe flash (see Figure 7 and text for explanation). The data points are fitted with a bell-shaped titration curve (solid line; see eq 5 in ref *46*) which yielded the p*K* values of about 4.5 and 8.0 in the acidic and alkaline regions, respectively.

reported for the pH dependence of the S_0 ML signal amplitude [Figure 6A, thin line, p*K*'s of 4.2 ± 0.2 and 8.0 ± 0.1 (*46*)]. This indicates that the $S_3 \rightarrow [S_4] \rightarrow S_0$ transition is blocked at both acidic and alkaline pH values.

Again, these data must be evaluated with care prior to defining the pH dependence. It is necessary to take into account both the pH dependence of the S_0 ML signal amplitude (*46*) and the decay of the S_0 centers during the 4 min dark incubation [due to the reaction $S_0Y_D^{\bullet} \rightarrow S_1Y_D$ (*42*)]. The latter reaction has two components decaying in the minutes and hours time scale, respectively. The half-time of the fast (minutes) component is about 48 min at pH 4.4 but decreases to about 8 min when the pH is elevated to 6.8 or above (*42*). Thus, the decay of S_0 is significant at the higher pHs. The calculated decay of the S_0 ML signal during the 4 min dark incubation is presented in the inset of Figure 6A.

The results of these corrections are shown in Figure 6B, which shows that the $S_3 \rightarrow [S_4] \rightarrow S_0$ transition is inhibited at both low and high pH. The data can be fitted well with

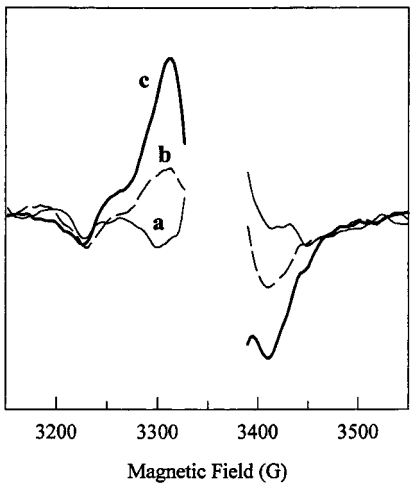

FIGURE 7: Results from an alternative experiment to determine the pH dependence of the $S_3 \rightarrow [S_4] \rightarrow S_0$ transition. The spectra show the induction of the $S_2Y_Z^{\bullet}$ split signal by two flashes, ΔpH_1, the probe flash, and ΔpH_2 to pH 8.3 (see text). The pH after the first pH change in this experiment was (a) pH 7.3, (b) pH 7.9, and (c) pH 8.2. To better visualize the $S_2Y_Z^{\bullet}$ split signal, the big underlying signal from $Y_D^{\bullet}$ has been subtracted. The $g \approx 2$ region has been excised for clarity. EPR settings: microwave power 25 mW; microwave frequency 9.40 GHz; temperature 7 K; modulation frequency 100 kHz; modulation amplitude 5 G.

protonation/deprotonation steps (see eq 5 in ref *46*) with $pK_1 \approx 4.5$ and $pK_2 \approx 8.0$, respectively.

We have recently found (*47*) that a 90−100 G wide $S_2Y_Z^{\bullet}$ split signal can be induced by a pH jump to pH 8.0 or above in the S_3 state (in our earlier study the pH jump was performed after two flashes). The p*K* of this $S_3 \rightarrow S_2Y_Z^{\bullet}$ conversion was 8.5 ± 0.3. The alkaline p*K* of the $S_3 \rightarrow [S_4] \rightarrow S_0$ transition, measured by the formation of the S_0 ML signal, occurred below this value ($pK_2 \approx 8.0$, Figure 6B). Therefore, we could also follow the disappearance (or absence of disappearance!) of the S_3 state at different pHs above pH 6.0 by using a special experimental protocol. In this protocol we applied a second pH change [after the sequence of two flashes, pH jump and probe flash (Scheme 2, panel C)] to elevate the pH to 8.3. The second pH move was applied to reveal the remaining S_3 state in the shape of the $S_2Y_Z^{\bullet}$ signal.

Figure 7 shows spectra from this experiment. After two flashes, ΔpH_1 to pH 7.3, the probe flash, and ΔpH_2 to pH 8.3 (Figure 7, spectrum a), there was no observable $S_2Y_Z^{\bullet}$ ("S_3") signal. This shows that the S_3 centers completely turned over to S_0 at pH 7.3. However, the same protocol with a ΔpH_1 to pH 7.9 (Figure 7, spectrum b) or 8.2 (Figure 7, spectrum c) induced a signal from $S_2Y_Z^{\bullet}$. The signal was bigger when the probe flash was applied at the higher pH. This shows that the $S_3 \rightarrow [S_4] \rightarrow S_0$ transition was inhibited at these pH values. This complex experiment was conducted at several alkaline pHs, and the formation of the $S_2Y_Z^{\bullet}$ split signal after two flashes, ΔpH_1, one flash, and ΔpH_2, occurred with $pK \approx 8.1$ (Figure 6B, black squares). This is in very good agreement with the result obtained by our measurements of the S_0 signal (Figure 6B, open circles; see above). Thus, this second experiment is particularly valuable since the S_0 ML signal studied in the first approach is very small in the alkaline region (Figure 5, spectra c and d; Figure 6), which is an inherent problem in our experiment. In our

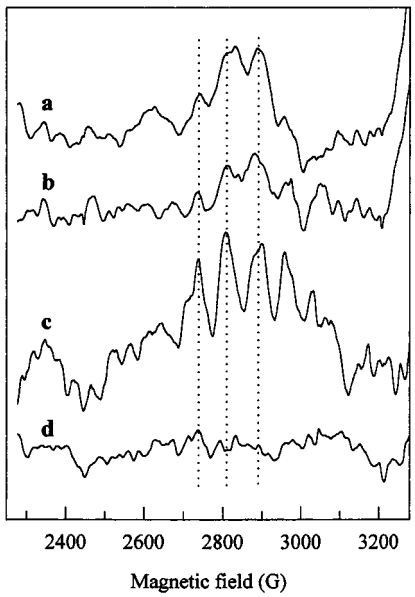

FIGURE 8: Low-field part of the S_0 state ML EPR signal induced by three flashes at pH 6.0 followed by either a pH jump (spectra a and c) or a pH jump and a probe flash (spectra b and d). The final pH was 4.6 (a and b) and 6.2 (c and d). The same samples were used for both experiment pairs. The probe flash was provided after the sample had been thawed after the first EPR measurements. A 4 min dark incubation was applied before the sample was frozen the first and second time to minimize the contribution of the S_2 ML signal. Any remaining S_2 ML signal has been subtracted from the spectra. (For raw spectra see Supporting Information.) The dotted lines indicate the three peaks used for the determination of the spectral intensities in Figure 9A. EPR settings as in Figure 5.

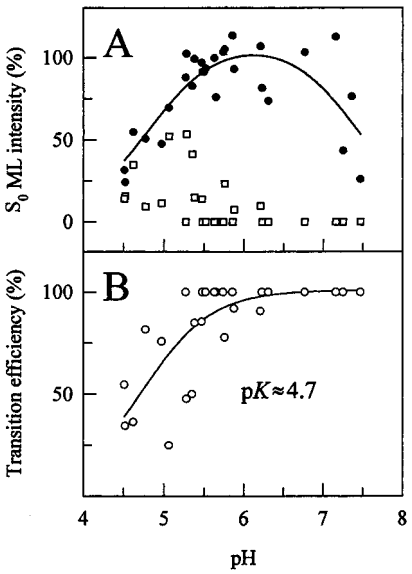

FIGURE 9: pH dependence of the $S_0 \rightarrow S_1$ transition. (A) pH dependence of the S_0 ML signal intensity. The S_0 ML signal was induced by three flashes followed by the pH jump (●) or remained after the subsequent probe flash (□). See Figure 8 for experimental conditions. The amplitudes were measured and compared as in Figures 5 and 6A except that the decay of the S_0 state was insignificant. (B) Efficiency of the $S_0 \rightarrow S_1$ transition as a function of pH. The data points (○) are obtained from panel A where the relative difference of the intensity before and after the probe flash at each pH (●, □) corresponds to the efficiency of the transition. The data points are fitted with a titration curve with one pK (solid line; see eq 1 in ref *47*) which yielded a pK value about of 4.7.

opinion, the similar results obtained by the two different protocols strengthen our results obtained by the complicated experimental protocols and data analysis.

pH Dependence of the $S_0 \rightarrow S_1$ Transition. The pH dependence of the $S_2 \rightarrow S_3$ transition was studied by the disappearance of the S_2 ML signal after the probe flash (see above). In a similar fashion, the decrease of the S_0 ML signal after the probe flash was used to study the $S_0 \rightarrow S_1$ transition (Scheme 2, panel D). The analysis was simpler for the $S_0 \rightarrow S_1$ transition, because the decay of the S_0 state is slow (at pH 6). This made it possible to use a 4 min dark incubation to eliminate the remaining S_3 population before the probe flash was given (see Table 1). This was necessary, since the probe flash otherwise could induce S_0 from the significant S_3 population after the third flash (≈33%, Table 1). In addition, the stability of the S_0 ML signal at pH ≤6 allowed us to use the same sample to measure the signal both before and after the probe flash. A second 4 min dark incubation was applied after the probe flash to decrease the S_2 ML signal contribution in the spectra. This would otherwise be large since there was a significant S_1 population prior to the probe flash.

Figure 8 shows two pairs of spectra, recorded at pH 4.6 (spectra a and b) and 6.2 (spectra c and d), after three flashes and a pH jump (spectra a and c) and after three flashes and a pH jump, followed by the probe flash (spectra b and d). The S_0 ML signal disappeared completely after the probe flash at pH 6.2 (spectrum d). In contrast, at pH 4.6, a significant fraction of the signal remained after the flash (spectrum b). This indicates that the $S_0 \rightarrow S_1$ transition is open at pH 6.2 but blocked at low pH.

The individual data points are shown in Figure 9A. The relative difference of the data points (between the filled circles and open squares) is characteristic for the $S_0 \rightarrow S_1$ transition at different pHs. The efficiency of the $S_0 \rightarrow S_1$ transition is shown in Figure 9B. The data points can be fitted by a simple titration curve with p$K \approx 4.7$. We should emphasize that in this experiment we did not have to correct our measurements for the pH-dependent amplitude of the S_0 ML signal (*46*) since the measurements before and after the probe flash were done at exactly the same pH. It is worth mentioning that we carried out similar experiments with two parallel sample series (independent samples frozen after the probe flash) and the same pK value was obtained (not shown).

Due to the small signal intensity, the S_0 signal cannot be used for studies above pH 7.5 to establish if there is a block at high(er) pH or not. Fortunately, the formation of the S_1 state centers can be followed by measuring the difference of the S_2 ML signal intensity before and after a subsequent illumination at 200 K, which oxidize the formed S_1 centers to the S_2 state (*61*, *65*).

Figure 10 shows four S_2 difference (±200 K illumination) ML spectra at pH 7.3 (spectra a and b) and 8.9 (spectra c and d) representing the S_1 populations before (spectra a and c) and after (spectrum b and d) the probe flash, respectively. There was an observable increase in the S_1 population after the probe flash even at pH 8.9 (Figure 10, spectrum d), indicating that the $S_0 \rightarrow S_1$ transition seems to be (at least partially) open at this pH. The individual data points are presented in Figure 11A. The relative difference between the data points is a direct measure of the efficiency of the $S_0 \rightarrow S_1$ transition over this pH range, as shown in Figure

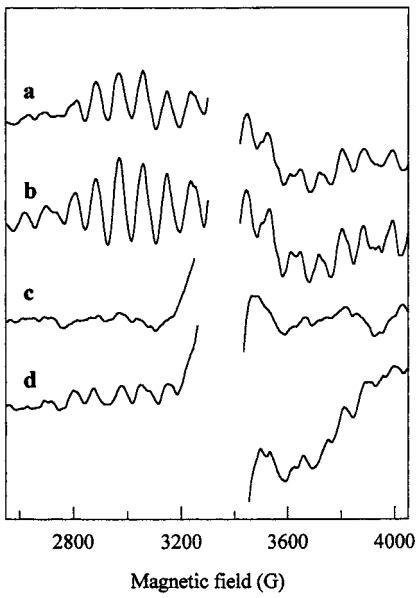

FIGURE 10: Analysis of the pH-dependent *formation* of the S_1 state during the $S_0 \rightarrow S_1$ transition. The PSII centers that reached the S_1 state with the probe flash after the pH change were converted to the S_2 state by illumination at 200 K. This allowed us to estimate the S_1 population from the intensity of the S_2 ML signal formed by the illumination at 200 K. The spectra represent the difference between the spectrum recorded after illumination at 200 K and the spectrum recorded before in samples exposed to three flashes followed by the pH jump (spectra a and c) or after a subsequent probe flash (spectra b and d). The final pH was 7.3 (spectra a and b) and 8.9 (spectra c and d). The $g \approx 2$ region has been excised for clarity. For EPR settings see Figure 1.

11B. Since the efficiency is 100% even at pH 8.9, it could be concluded that the $S_0 \rightarrow S_1$ transition is open in the alkaline pH range. Thus, the theoretical alkaline block (if there is any) is at very high pH ($\geq$10.0).

Comparison of the pH Dependence of the Individual S-State Transitions and the Steady-State Oxygen Evolution. It is worthwhile to compare the pH dependence of the individual S-transitions and the pH dependence of the steady-state oxygen evolution, which, depending on the PSII preparation procedure, shows half-inhibition values between pH 4.8−5.5 and pH 7.4−8.0 (*42*, *43*). In our PSII preparation in the presence of 5% methanol (v/v) (*58*), we found that the oxygen evolution (Figure 12A, open circles) is inhibited with half-inhibition values around pH 4.8 and 8.0. This is identical to the pH dependence in the absence of methanol (Figure 12A, filled circles). Multiplication of the functions describing the pH dependence of the individual S-state transitions reveals the efficiency of the whole cycle as a function of pH and, consequently, of the oxygen evolution if the pH dependence is dominated by the S-cycle. This calculation (Figure 12B) resulted in a titration curve for the oxygen evolution with half-inhibition values at pH 5.0 and 8.0. This is in remarkably good agreement with the inhibition of the steady-state oxygen evolution.

This analysis shows that the decrease of the steady-state oxygen evolution at low pH is a consequence of the simultaneous inhibition of three of the S-transitions. In contrast, at high pH the inhibition of the oxygen evolution is almost completely determined by the inhibition of the $S_3 \rightarrow [S_4] \rightarrow S_0$ transition.

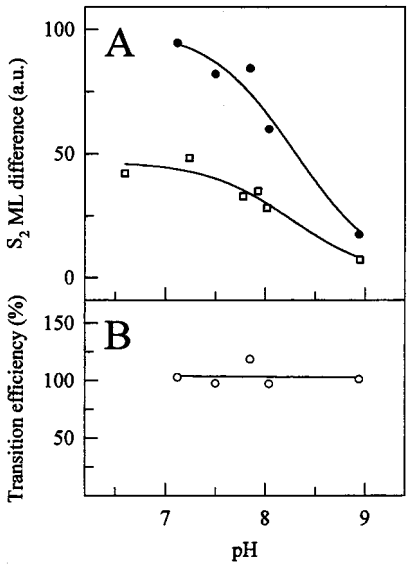

FIGURE 11: An alternative protocol to determine the pH dependence of the $S_0 \rightarrow S_1$ transition at alkaline pH. (A) pH dependence of the S_2 ML spectra induced by 200 K illumination from PSII centers poised in the S_1 state either after three saturating laser flashes followed by the pH jump (□) or after also the subsequent probe flash (●). The amplitudes were measured and compared as in Figures 1 and 2A. The data points are fitted with a bell-shaped titration curve (see eq 5 in ref *46*). (B) Efficiency of the $S_0 \rightarrow S_1$ transition as a function of pH. The data points (○) are obtained from panel A by using the difference of the two sets of points (●, □) and normalizing this difference to the corrected S_2 ML signal amplitude titration curve (Figure 2A, thin line, and ref *46*). The points were fitted with a linear function.

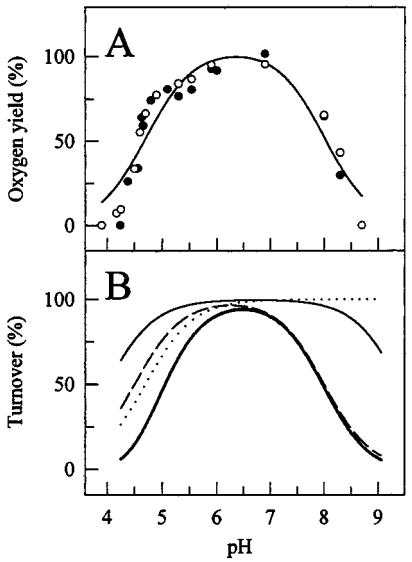

FIGURE 12: pH dependence of the whole S-cycle. (A) Steady-state oxygen evolution at different pHs measured in the presence (○) or absence (●) of 5% methanol (v/v). The maximal oxygen evolution at pH 6.5 [$\approx$400 μmol of O_2 (mg of Chl)$^{-1}$ h^{-1}] was considered to be 100%. (B) Multiplication of the titration curves, described by eq 5 in ref *46*, belonging to the three pH-dependent S-transitions: $S_2 \rightarrow S_3$ (p$K_1 \approx$ 4.0; p$K_2 \approx$ 9.4; thin solid line), $S_3 \rightarrow S_0$ (p$K_1 \approx$ 4.5; p$K_2 \approx$ 8.0; dashed line), and $S_0 \rightarrow S_1$ (p$K \approx$ 4.7; dotted line). The product of their multiplication (thick line) gives the pH dependence of the whole S-cycle.

DISCUSSION

First in the discussion we should discuss the precision in our measurements. To allow efficient turnover, we are forced

to work with weak concentrations of PSII membranes as compared to many other EPR investigations. This makes our studied ML EPR signals small. However, our experiment is made possible since we use the very sensitive SHQ cavity which makes our signal to noise ratio much better than in our earlier studies of the S_2 and S_0 ML signals (*46*, *48*, *51*). Both the S_2 and S_0 ML signals are decreased in size at alkaline and acidic pHs. Despite this, the S_2 ML signal is large enough to be measured accurately in the entire pH interval from 3.9−8.9. The situation is different for the S_0 ML signal, which is much smaller at all pHs (*48*, *51*). This makes our precision lower both at alkaline and at acidic pHs. Partially we have overcome this by measuring many samples in many independent series. Despite this, our precision is lower in the transitions where the S_0 signal was our spectral probe ($S_3 \rightarrow [S_4] \rightarrow S_0$ and $S_0 \rightarrow S_1$) than in the transitions where the S_2 ML signal was measured ($S_1 \rightarrow S_2$ and $S_2 \rightarrow S_3$).

We feel that our data are as good as can be produced. The amplitudes of the ML signals are inherently small at the extreme pHs. We have also applied complex experimental protocols and much data treatment, which makes the true error in the data difficult to ascertain. We have therefore chosen not to provide error estimations of our determined p*K*'s. In most cases the inhibition (or absence of inhibition) is clear. We also trust the conclusion that the acidic p*K* for the inhibition of $S_2 \rightarrow S_3$ is lower than that of $S_3 \rightarrow [S_4] \rightarrow S_0$ which is lower that that of $S_0 \rightarrow S_1$ (Table 2). It is also clear that the weakest p*K* assignment is the alkaline block of the $S_2 \rightarrow S_3$ transition (p$K \approx 9.4$), which could only be partially studied.

Table 2: pH-Dependent Inhibition of the Individual Steps in the S-Cycle[a]

transition	pK_1[b]	pK_2[b]
$S_1 \rightarrow S_2$	pH independent	pH independent
$S_2 \rightarrow S_3$	4.0	9.4
$S_3 \rightarrow [S_4] \rightarrow S_0$	4.5	8.0
$S_0 \rightarrow S_1$	4.7	pH independent

[a] The p*K* values are given without error estimation. This was necessary since the errors cannot be estimated due to the combination of very complex experimental protocols and very small EPR signals at the extreme pHs (see text for discussion). [b] pK_1 and pK_2 are the p*K* for the inhibition in the acidic and alkaline regions, respectively.

Table 2 summarizes the pH dependence of the four redox transitions in the oxygen evolving S-cycle studied by our single flash technique. The $S_0 \rightarrow S_1$ transition is blocked with p$K \approx 4.7$ in the acidic region while it is open at least up to pH 10. The $S_1 \rightarrow S_2$ transition is not affected by the pH. It is fully operational between pH 4.1 and pH 8.4. The $S_2 \rightarrow S_3$ transition is inhibited with p$K_1 \approx 4.0$ in the acidic region and p$K_2 \approx 9.4$ in the alkaline region. The most distinct inhibition pattern is found for the $S_3 \rightarrow [S_4] \rightarrow S_0$ transition, which shows well-defined pH-dependent blocks both at acidic pH (p$K_1 \approx 4.5$) and at alkaline pH (p$K_2 \approx 8.0$). Our simulation of how these S-state transition inhibition profiles contribute to the overall pH dependence of steady-state oxygen evolution (Figure 12) shows that the oxygen evolution in PSII-enriched membranes is mainly influenced by pH modulations at the Mn_4 cluster and Y_Z while the acceptor side (at least in the presence of P*p*BQ as electron acceptor) has less influence. This emphasizes the importance of the proton concentration in the lumen for the function of PSII. When the leaf is exposed to light, the pH rapidly drops in the lumen where the OEC is located. Our results indicate that PSII is blocked at the level of individual S-transitions in a pH range easily reached under physiological conditions.

There is a vast literature on the proton release pattern in the S-cycle and how pH affects the function of various redox components in PSII. Our results here have importance for the interpretations in many of these studies. However, we find it too early to discuss all of these aspects at this stage. Instead, we will restrict our discussion to mechanisms that can explain the inhibition of certain S-state transitions at low and high pH. We will also speculate somewhat on why the $S_1 \rightarrow S_2$ transition is pH independent.

The inhibition at low pH occurs with p$K \approx 4.0-4.7$ and seems to be similar in each S-transition except in the $S_1 \rightarrow S_2$ transition. We see two different mechanisms that can give rise to this inhibition pattern. Y_Z is connected to a hydrogen bond network that probably involves His190 (on the D1 protein) (*9*−*14*, *16*, *19*−*23*) and one or several carboxylic residues. The latter have not been identified, but many groups including ours (*9*, *13*, *19*−*21*, *66*, *67*) have suggested that D1-Glu189 can be one of these. It was recently found that the midpoint potential of the $Y_Z^{\bullet}/Y_Z$ couple can be titrated by changing the pH in the buffer. The interpretation from these results was that the hydrogen bond network extends from Y_Z to the solvent (*47*). It was furthermore suggested that this hydrogen bond network in fact is the proton release pathway in PSII and that proton release consequently is triggered upon the oxidation of Y_Z [similar to what has been suggested by Babcock and co-workers (*15*, *16*, *18*−*21*)].

It is not unlikely that one or several carboxylic residue(s) is (are) the point of contact between the hydrogen bond network and the solvent (*47*). Carboxylic amino acids normally become protonated with p*K*'s around 4.5. Protonation of a proton release site would close the proton release pathway from Y_Z, thereby preventing turnover of the OEC. The protonation of the pathway would possibly also *increase* the midpoint potential of the $Y_Z^{\bullet}/Y_Z$ couple. The $Y_Z^{\bullet}/Y_Z$ potential then could become close to the available oxidizing potential of the $P680^+/P680$ pair below pH 4−4.5 (*47*). This would slow or prevent oxidation of Y_Z at very low pHs. This could explain our inhibitory pattern.

It has also been proposed that the low pH actually induces a Ca^{2+} release from its site in the OEC (*68*−*70*). This would explain a block in the S-cycle between S_2 and S_3, which is often thought to be the site for inhibition due to Ca^{2+} depletion (ref *6* and references cited therein). It is less obvious how it would affect the other transitions that are blocked at low pH ($S_0 \rightarrow S_1$ and $S_3 \rightarrow [S_4] \rightarrow S_0$). However, it is unlikely that our conditions would give rise to release of Ca^{2+} from the OEC. In our experience, Ca^{2+} depletion is achieved at pH 3.0 in the presence of a chelator that binds Ca^{2+} (5 min treatment; refs *57* and *71*) and not at pH 4−5 for 30 s in the presence of 5 mM $CaCl_2$ (our conditions; see Materials and Methods).

We are thus of the opinion that the inhibition at low pH rather reflects protonation of one or several carboxylic residues in the proton release pathway from the OEC. The most likely candidate is a carboxylic residue close to Y_Z and D1-His190. The pH titration of the $P680^+$ reduction kinetics

(*13*, *26*, *72*, *73*) and deuterium isotope effects on the pH-dependent $P680^+$ reduction (*74*) support this idea.

The inhibition at alkaline pH is probably easier to explain. We recently found that a pH jump in the S_3 state induced the formation of the $S_2Y_Z^\bullet$ state (*47*). We proposed that this reflected a pH-induced shift of the redox potential of the $Y_Z^\bullet/Y_Z$ couple, making it less oxidizing than the S_3/S_2 couple of the Mn cluster.

We propose that this mechanism applies to the $Y_Z^\bullet/Y_Z$ couple in all S-states. It explains well the inhibition of the $S_3 \rightarrow [S_4] \rightarrow S_0$ transition since $Y_Z^\bullet$ cannot oxidize the S_3 state above pH 8−8.5 fast enough to avoid side reactions leading to reduction of $Y_Z^\bullet$. In contrast, both the S_0 and the S_1 states are low enough in potential so that they can be oxidized by $Y_Z^\bullet$ even at high pH [the oxidizing potential of the $Y_Z^\bullet/Y_Z$ couple approaches +800 mV even at pH 8.5 (see Figure 8 in ref *47*)]. Thus, there is no alkaline block in the $S_0 \rightarrow S_1$ and $S_1 \rightarrow S_2$ transitions. The situation is less clear for the $S_2 \rightarrow S_3$ transition, which was found to be blocked with p$K \approx 9.4$. The S_2 state is considered to be about 50 mV less oxidizing than $Y_Z^\bullet$ at pH 6−7 (*42*, *75*). This would mean that $Y_Z^\bullet$ would become unable to oxidize the S_2 state above pH ≈8 if the oxidizing potential of the S_2 state was unaffected by pH. We find, however, that the $S_2 \rightarrow S_3$ transition is inhibited with p$K \approx 9.4$. A simple explanation to this is that the redox potential of the S_2/S_1 state is pH dependent in parallel to the $Y_Z^\bullet/Y_Z$ couple. This idea is similar to what was proposed earlier from different arguments (*47*).

One further aspect of our results should be discussed. Why is the $S_1 \rightarrow S_2$ transition independent of pH over the whole studied pH interval? As discussed above, the proposed titration of the midpoint potential of the $Y_Z^\bullet/Y_Z$ couple can explain the lack of a block on the alkaline side. The midpoint potential of the $Y_Z^\bullet/Y_Z$ couple can be expected to be higher than the S_1 redox potential also at elevated pHs.

However, it less obvious why there is no block on the acidic side in the $S_1 \rightarrow S_2$ transition which otherwise affects all (both high potential and low redox potential) S-transitions similarly. The proton release pattern in the $S_1 \rightarrow S_2$ transition is complex and difficult to measure. In PSII-enriched membranes, the proton release in the first flash was not measured due to experimental complications (*33*, *34*), and the proton release in the $S_1 \rightarrow S_2$ transition was studied only in the fifth flash. It was found that no protons were released below pH 5.5 and that about 0.5−0.8 proton was released in a pH-dependent manner above pH 6.5. If this proton release pattern also applies for the first flash (corresponding to our conditions), the lack of proton release below pH 5.5 explains the pH independence of this transition also below pH 5.

ACKNOWLEDGMENT

The authors acknowledge stimulating discussions with Paulina Geijer, Warwick Hillier, and Fikret Mamedov and invaluable help from Ms. Emelie Styring in preparing the manuscript.

SUPPORTING INFORMATION AVAILABLE

Two figures showing the raw spectra, containing both the S_2 ML signal (from a fraction of centers) and the S_0 ML signal, used to produce the "pure" S_0 ML spectra to determine the pK's for the $S_3 \rightarrow S_0$ and $S_3 \rightarrow S_0$ transition, the pure S_0 spectra being derived by subtraction of the contaminating S_2 ML contribution. This material is available free of charge via the Internet at http://pubs.acs.org.

REFERENCES

1. Zouni, A., Witt, H. T., Kern, J., Fromme, P., Krauss, N., Saenger, W., and Orth, P. (2001) *Nature 409*, 739−743.
2. Rhee, K.-H., Morris, E. P., Barber, J., and Kühlbrandt, W. (1998) *Nature 396*, 283−286.
3. Diner, B. A., and Babcock, G. T. (1996) in *Oxygenic Photosynthesis: The Light Reactions* (Ort, D. R., and Yocum, C. F., Eds.) pp 249−264, Kluwer Academic Publishers, Dordrecht, The Netherlands.
4. Barber, J., and Andersson, B. (1994) *Nature 370*, 31−34.
5. Magnuson, A., Frapart, Y., Abrahamsson, M., Horner, O., Åkermark, B., Sun, L., Girerd, J.-J., Hammarström, L., and Styring, S. (1999) *J. Am. Chem. Soc. 121*, 89−96.
6. Debus, R. J. (1992) *Biochim. Biophys. Acta 1102*, 269−352.
7. Debus, R. J. (2000) in *Manganese and Its Role in Biological Processes* (Sigel, A., and Sigel, H., Eds.) pp 657−711, Marcel Dekker, Basel, Switzerland.
8. Britt, R. D. (1996) in *Oxygenic Photosynthesis: The Light Reactions* (Ort, D. R., and Yocum, C. F., Eds.) pp 137−164, Kluwer Academic Publishers, Dordrecht, The Netherlands.
9. Svensson, B., Etchebest, C., Tuffery, P., van Kan, P., Smith, J., and Styring, S. (1996) *Biochemistry 35*, 14486−14502.
10. Mamedov, F., Sayre, R. T., and Styring, S. (1998) *Biochemistry 37*, 14245−14256.
11. Hays, A.-M. A., Vassiliev, I. R., Golbeck, J. H., and Debus, R. J. (1998) *Biochemistry 37*, 11352−11365.
12. Hays, A.-M. A., Vassiliev, I. R., Golbeck, J. H., and Debus, R. J. (1999) *Biochemistry 38*, 11851−11865.
13. Christen, G., Seeliger, A., and Renger, G. (1999) *Biochemistry 38*, 6082−6092.
14. Debus, R. J. (2001) *Biochim. Biophys. Acta 1503*, 164−186.
15. Hoganson, C. W., Lydakis-Simantiris, N., Tang, X.-S., Tommos, C., Warncke, K., Babcock, G. T., Diner, B. A., McCracken, J., and Styring, S. (1995) *Photosynth. Res. 46*, 177−184.
16. Tommos, C., Tang, X.-S., Warncke, K., Hoganson, C. W., Styring, S., McCracken, J., Diner, B. A., and Babcock, G. T. (1995) *J. Am. Chem. Soc. 117*, 10325−10335.
17. Gilchrist, M. L., Ball, J. A., Randall, D. W., and Britt, R. D. (1995) *Proc. Natl. Acad. Sci. U.S.A. 92*, 9545−9549.
18. Hoganson, W. C., and Babcock, G. T. (1997) *Science 277*, 1953−1956.
19. Tommos, C., and Babcock, G. T. (1998) *Acc. Chem. Res. 31*, 18−25.
20. Tommos, C., and Babcock, G. T. (2000) *Biochim. Biophys. Acta 1458*, 199−219.
21. Hoganson, C. W., and Babcock, G. T. (2000) in *Manganese and Its Role in Biological Processes* (Sigel, A., and Sigel, H., Eds.) pp 613−656, Marcel Dekker, Basel, Switzerland.
22. Vrettos, J. S., Limburg, J., and Brudvig, G. W. (2001) *Biochim. Biophys. Acta 1503*, 229−245.
23. Renger, G. (2001) *Biochim. Biophys. Acta 1503*, 210−228.
24. Haumann, M., and Junge, W. (1999) *Biochim. Biophys. Acta 1411*, 86−91.
25. Rappaport, F., and Lavergne, J. (1997) *Biochemistry 36*, 15294−15302.
26. Ahlbrink, R., Haumann, M., Cherepanov, D., Bögerhausen, O., Mulkidjanian, A., and Junge, W. (1998) *Biochemistry 37*, 1131−1141.
27. Kok, B., Forbush, B., and McGloin, M. (1970) *Photochem. Photobiol. 11*, 457−475.
28. Saphon, S., and Crofts, A. (1977) *Z. Naturforsch. 32C*, 617−626.
29. Schlodder, E., and Witt, H. T. (1999) *J. Biol. Chem. 274*, 30387−30392.
30. Lavergne, J., and Junge, W. (1993) *Photosynth. Res. 38*, 279−296.

31. Lübbers, K., Haumann, M., and Junge, W. (1993) *Biochim. Biophys. Acta 1183*, 210−214.
32. Haumann, M., and Junge, W. (1996) in *Oxygenic Photosynthesis: The Light Reactions* (Ort, D. R., and Yocum, C. F., Eds.) pp 165−192, Kluwer Academic Publishers, Dordrecht, The Netherlands.
33. Haumann, M., Hundelt, M., Jahns, P., Chroni, S., Bögerhausen, O., Ghanotakis, D., and Junge, W. (1997) *FEBS Lett. 410*, 243−248.
34. Rappaport, F., and Lavergne, J. (1991) *Biochemistry 30*, 10004−10012.
35. Haumann, M., and Junge, W. (1994) *Biochemistry 33*, 864−872.
36. Force, D. A., Randall, D. W., and Britt, R. D. (1997) *Biochemistry 36*, 12062−12070.
37. Tang, X.-S., Randall, D. W. Force, D. A., Diner, B. A., and Britt, R. D. (1996) *J. Am. Chem. Soc. 118*, 7638−7639.
38. Bögerhausen, O., and Junge, W. (1995) *Biochim. Biophys. Acta 1230*, 177−185.
39. Nugent, J. H. A., Rich, A. M., and Evans, M. C. W. (2001) *Biochim. Biophys. Acta 1503*, 138−146.
40. Candeias, L. P., Turconi, S., and Nugent, J. H. A. (1998) *Biochim. Biophys. Acta 1363*, 1−5.
41. Limburg, J., Szalai, V. A., and Brudvig, G. W. (1999) *J. Chem. Soc., Dalton Trans.*, 1353−1361.
42. Vass, I., and Styring, S. (1991) *Biochemistry 30*, 830−839.
43. Damoder, R., and Dismukes, G. C. (1984) *FEBS Lett. 174*, 157−161.
44. Messinger, J., and Renger, G. (1994) *Biochemistry 33*, 10896−10905.
45. Vass, I., Koike, H., and Inoue, Y. (1985) *Biochim. Biophys. Acta 810*, 302−309.
46. Geijer, P., Deák, Z., and Styring, S. (2000) *Biochemistry 39*, 6763−6772.
47. Geijer, P., Morvaridi, F., and Styring, S. (2001) *Biochemistry 40*, 10881−10891.
48. Åhrling, K. A., Peterson, S., and Styring, S. (1997) *Biochemistry 36*, 13148−13152.
49. Messinger, J., Nugent, J. H. A., and Evans, M. C. W. (1997) *Biochemistry 36*, 11055−11060.
50. Messinger, J., Robblee, J., Yu, W. O., Sauer, K., Yachandra, V. K., and Klein, M. P. (1997) *J. Am. Chem. Soc. 119*, 11349−11350.
51. Åhrling, K. A., Peterson, S., and Styring, S. (1998) *Biochemistry 37*, 8115−8120.
52. Dismukes, G. C., and Siderer, Y. (1981) *Proc. Natl. Acad. Sci. U.S.A. 78*, 274−278.
53. Miller, A.-F., and Brudvig, G. W. (1991) *Biochim. Biophys. Acta 1056*, 1−18.
54. Geijer, P., Peterson, S., Åhrling, K. A., Deák, Z., and Styring, S. (2001) *Biochim. Biophys. Acta 1503*, 83−95.
55. Boussac, A., Zimmermann, J.-L., and Rutherford, A. W. (1989) *Biochemistry 28*, 8984−8989.
56. Sivaraja, M., Tso, J., and Dismukes, G. C. (1989) *Biochemistry 28*, 9459−9464.
57. Ono, T.-a., and Inoue, Y. (1989) *Biochim. Biophys. Acta 973*, 443−449.
58. Pace, R. J., Smith, P., Bramley, R., and Stehlik, D. (1991) *Biochim. Biophys. Acta 1058*, 161−170.
59. Arnon, D. I. (1949) *Plant. Physiol. 24*, 1−15.
60. Deák, Z., Peterson, S., Geijer, P., Åhrling, K. A., and Styring, S. (1999) *Biochim. Biophys. Acta 1412*, 240−249
61. Styring, S., and Rutherford, A. W. (1988) *Biochim. Biophys. Acta 933*, 378−387.
62. Styring, S., and Rutherford, A. W. (1988) *Biochemistry 27*, 4915−4923.
63. Evelo, R. G., Styring, S., Rutherford, A. W., and Hoff, A. J. (1989) *Biochim. Biophys. Acta 973*, 428−442.
64. Cole, J., Boska, M., Blough, N. V., and Sauer, K. (1986) *Biochim. Biophys. Acta 848*, 41−47.
65. Brudvig, G. W., Casey, J. L., and Sauer, K. (1983) *Biochim. Biophys. Acta 723*, 366−371.
66. Chu, H.-A., Nguyen, A. P., and Debus, R. J. (1995) *Biochemistry 34*, 5839−5858.
67. Haumann, M., and Junge, W. (1999) *Biochim. Biophys Acta 1411*, 121−133.
68. Krieger, A., and Weis, E. (1992) *Photosynthetica 27*, 89−98.
69. Krieger, A., and Weis, E. (1993) *Photosynth. Res. 37*, 117−130.
70. Krieger, A., Weis, E., and Demeter, S. (1993) *Biochim. Biophys. Acta 1144*, 411−418.
71. Ono, T.-a., and Inoue, Y. (1988) *FEBS Lett. 227*, 147−152.
72. Schlodder, E., and Meyer, B. (1987) *Biochim. Biophys. Acta 890*, 23−31.
73. Meyer, B., Schlodder, E., Dekker, J. P., and Witt, H. T. (1989) *Biochim. Biophys. Acta 974*, 36−43.
74. Diner, B. A., Force, D. A., Randall, D. W., and Britt, R. D. (1998) *Biochemistry 37*, 17931−17943.
75. Vos, M. H. (1990) Ph.D. Thesis, University of Leiden, Leiden, The Netherlands.

BI011691U